3 Biotech (2024) 14:189
https://doi.org/10.1007/s13205-024-04029-z

ORIGINAL ARTICLE

New biocatalyst produced from fermented biomass: improvement of adsorptive characteristics and application in aroma synthesis

Márcia Soares Gonçalves[1] · Iasnaia Maria de Carvalho Tavares[1] · Igor Carvalho Fontes Sampaio[3] · Marta Maria Oliveira dos Santos[2] · Helen Luiza Brandão Silva Ambrósio[3] · Sabryna Couto Araújo[3] · Cristiane Martins Veloso[4] · Jaci Lima Vilanova Neta[3] · Adriano Aguiar Mendes[5] · Paulo Neilson Marques dos Anjos[7] · Héctor A. Ruiz[6] · Marcelo Franco[3]

Received: 27 January 2024 / Accepted: 14 July 2024 / Published online: 30 July 2024

Abstract

This study presents a novel approach to producing activated carbon from agro-industrial residues, specifically cocoa fruit peel, using solid-state fermentation (SSF) with *Aspergillus niger*. The process effectively degrades lignin, a major impediment in traditional activated carbon production, resulting in a high-quality carbon material. This carbon was successfully utilized for enzyme immobilization and aroma synthesis, showcasing its potential as a versatile biocatalyst. The study meticulously evaluated the physical and chemical attributes of activated carbon derived from fermented cocoa peel, alongside the immobilized enzymes. Employing a suite of analytical techniques—electrophoresis, FTIR, XRD, and TG/DTG the research revealed that fermentation yields a porous material with an expansive surface area of 1107.87 m^2/g. This material proves to be an excellent medium for lipase immobilization. The biocatalyst fashioned from the fermented biomass exhibited a notable increase in protein content (13% w/w), hydrolytic activity (15% w/w), and specific activity (29% w/w), underscoring the efficacy of the fermentation process. The significant outcome of this research is the development of a sustainable method for activated carbon production that not only overcomes the limitations posed by lignin but also enhances enzyme immobilization for industrial applications. The study's findings have important implications for the agro-industrial sector, promoting a circular economy and advancing sustainable biotechnological processes.

Keywords Activated carbon · *Aspergillus niger* · Enzymatic catalysis · Solid state fermentation · Lignocellulosic residue

Abbreviations

AC	Activated carbon
ACC	Activated carbon from cocoa husk without SSF
ACCAn	Activated carbon from cocoa husk with *Aspergillus niger*
ACCAnI	Activated carbon from cocoa husk with *Aspergillus niger* with immobilized LLP
ACCI	Activated carbon from cocoa husk with immobilized LLP
CCAn	Cocoa husk after SSF with *Aspergillus niger*

✉ Marcelo Franco
mfranco@uesc.br
https://www.researchgate.net/profile/Marcelo-Franco-2
https://publons.com/researcher/1288618/marcelo-franco/
https://scholar.google.com/citations?view_op=list_works&hl=pt-BR&user=ERlVXQoAAAAJ

[1] Department of Exact and Natural Sciences, State University of Southwest, Itapetinga 45700-000, Brazil

[2] Post-Graduation Institute of Chemistry and Biotechnology, Federal University of Alagoas, A. C. Simões Campus, Maceió, Alagoas 57072-900, Brazil

[3] Biotransformation and Organic Biocatalysis Research Group, Department of Exact Sciences (DCEX), State University of Santa Cruz (UESC), Ilhéus, Bahia 45662-900, Brazil

[4] Process Engineering Laboratory, State University of Southwest, Itapetinga 45700-000, Brazil

[5] Institute of Chemistry, Federal University of Alfenas, Alfenas 37130-001, Brazil

[6] Biorefinery Group, Food Research Department, School of Chemistry, Autonomous University of Coahuila, 25280 Saltillo, Coahuila, Mexico

[7] Laboratory of Research and Innovation of Advanced Materials, Department of Exact Sciences, Santa Cruz State University, Ilhéus 45654-370, Brazil

CFC	Cocoa husk without SSF
DRX	X-ray diphatrometry
DTG	Derived from thermogravimetric analysis
HA	Hydrolytic activity
IP	Immobilized protein
PPL	Porcine pancreas lipase
SA	Specific activity
SACC	Supernatant after immobilization on cocoa husk activated carbon
SCAAn	Supernatant after immobilization Activated carbon from cocoa husks after SSF with *Aspergillus niger*
SSF	Solid state fermentation
TG	Thermogravimetric analysis

Introduction

The accumulation of agricultural waste poses significant environmental, social, and economic challenges globally, with Brazil being no exception. Effective management strategies for waste disposal remain underdeveloped (Veloso et al. 2020). In 2020, it was estimated that worldwide agricultural waste reached 375 million tons. As the world's third-largest agricultural producer, Brazil contributed approximately 263 million tons to this total (FAO 2020). Specifically, the cocoa industry, integral to chocolate production, alone produces an estimated 1.2 million tons of husks each year (Lu et al. 2018). Despite the vast potential for these by-products, their utilization remains largely unexplored and underutilized.

Given Brazil's position as the world's sixth-largest cocoa producer, extensive research has been conducted to explore the potential uses of cocoa residue. These studies focus on the residue's economic and environmental advantages (Lizardi-Jiménez and Hernández-Martínez 2017; Selo et al. 2021).

Solid-state fermentation (SSF) with *Penicillium roqueforti* ATCC 10110 has been instrumental in producing various crude enzymes, including lipases, β-glucosidase, endoglucanases, exoglucanase, xylanase, and proteases, as evidenced by numerous studies (Araujo et al. 2022; de Menezes et al. 2022a, b; Menezes et al. 2021; Silva et al. 2017; Soares et al. 2022; Neves et al. 2022; Oliveira et al. 2018; Nunes et al. 2020; Santos 2011; Ferraz et al. 2019; Souza et al. 2018; Nogueira et al. 2022). Similarly, *Aspergillus oryzae* ATCC 10124 and *Thermomyces lanuginosus* have been used for xylanase production, while *Aspergillus oryzae* has been noted for endoglucanase and xylanase production (de Carvalho et al. 2023; Reis et al. 2020). However, it's important to recognize that SSF also generates new residues. Addressing this, research into the valorization of these fermented biomasses has highlighted their potential in activated carbon production, thus reintegrating what would otherwise be waste back into the economic cycle. This aligns with the circular bioeconomy's goal of efficient natural resource management, maintaining the utility and value of products, components, and materials within a sustainable economic framework (Voukkali et al. 2023).

Aspergillus niger was selected for this study due to its well-documented efficacy in solid-state fermentation (SSF), which offers advantages such as simplicity, lower production costs, high enzyme yields, and low wastewater output. Its ability to degrade lignin effectively makes it an ideal candidate for producing high-quality activated carbon from cocoa fruit peel, a process that is further enhanced by the fungus's robust enzymatic activity. This choice aligns with the study's goal of developing a sustainable and economically viable method for activated carbon production, contributing to the circular economy and advancing biotechnological processes (Santos et al. 2011, 2016; Gonçalves et al. 2024).

Contemporary literature documents the utilization of activated carbon (AC) for enzyme immobilization, employing agro-industrial residues like cocoa husk and siriguela seed (Pereira et al. 2014), cajá core (Brito et al. 2017), and rice husk (Gama et al. 2019). Notably absent, however, is the application of residual fermented biomass from Solid-State Fermentation (SSF) in such processes. Recent findings by Lessa et al. (2023) indicate that SSF, particularly when induced by filamentous fungi, engenders structural alterations in cocoa husk fibers. These alterations diminish amorphous constituents such as lignin, enhancing the activated carbon's textural properties, surface area, and porosity (Santos et al. 2020). Such modifications are poised to beneficially modulate the kinetic parameters of immobilized enzymes, thereby augmenting biocatalyst stability and facilitating efficient industrial deployment (Costa-Silva et al. 2022). Ruiz et al. (2021) underscore the pivotal role of stability in the commercial viability of biocatalysts, including lipases, throughout their operational and storage phases.

The immobilization process is instrumental in optimizing lipase catalysis, leveraging a surface activation mechanism that repositions a hydrophobic polypeptide chain, thus exposing the active site to hydrophobic substrates (Barbosa et al. 2013). This mechanism significantly enhances enzymatic activity, selectivity, specificity, and stability, while mitigating inhibition by reaction products (Arana-Peña et al. 2022). The success of this strategy, yielding immobilized derivatives with heightened enzymatic activity and superior properties, is contingent upon the enzyme type, immobilization technique, and choice of support (Costa-Silva et al. 2022). Given the environmental and safety considerations, coupled with the prohibitive costs of conventional immobilization supports (Menezes et al. 2022a, b), exploiting residual fermented biomass as a precursor for activated carbon and

as a prospective enzyme immobilization matrix is highly advantageous.

The immobilized biocatalyst's utility in ester synthesis is particularly relevant, considering the substantial demand within the food, cosmetic, and pharmaceutical sectors. The flavoring industry, valued at 29 billion dollars in 2021, is anticipated to witness a 30% expansion by 2026 (Markets and Markets 2022). This growth trajectory is reflected in the widespread flavoring of diverse consumables, ranging from syrups and soft drinks (Liang et al. 2021) to baked goods like bread, cakes, and cookies (Khanna et al. 2021).

These compounds can be synthesized chemically or extracted from natural products. However, at an industrial scale, both methods have disadvantages, such as low yield and high costs (Sá et al. 2017; Mendes 2019). Conversely, producing aromas through an enzymatic route is a promising alternative, offering not only low costs and high productivity but also mild production conditions without the need for potentially toxic catalysts (Costa-Silva et al. 2022).

This study aims to harness the potential of fermented cocoa husk biomass via solid-state fermentation by Aspergillus niger for the innovative production of activated carbon. It further investigates the carbon's effectiveness as a support for enzyme immobilization in synthesizing the ester hexyl butyrate, which is pivotal for apple peel and citrus aromas. This research could significantly contribute to sustainable waste management practices and the advancement of green chemistry in flavor and fragrance industries.

Materials and methods

Materials, microorganism and inoculum

Porcine pancreatic lipase type II (PPL) and bovine serum albumin (BSA) were purchased from Sigma Aldrich Chemical Co. (St. Louis, MO, EUA). Low-acidity olive oil from Córdoba, Spain, was purchased at a local store in Itabuna, Bahia, Brazil. Butyric acid and hexanol were purchased from Synth® (São Paulo/SP, Brazil). All Other reagentes were obtained by Vetec Química (São Paulo/SP, Brazil). The shell of coca fruit (*Theobroma cacao*) was provided by CEPLAC (Executive Committee for Planning the Cocoa Farm located in Itabuna/BA, Brazil). The fungus *Aspergillus niger* ATCC 1004 was provided by Fundação Oswaldo (FIOCRUZ, Rio de Janeiro/RJ, Brazil) and duly deposited at the National Institute for Health Quality Control (INCQS, Rio de Janeiro/RJ, Brazil). The fungus was preserved in silica and glycerol and stored at − 80 °C in the ultrafreezer (UBXT-L-96, Tectalmaq, Piracicaba/SP, Brasil). Spore collections were cultured with Tween 80 solution. Spore counts were performed with a double-mirrored Neubauer Chamber and a binocular microscope (BIOVAL L1000, São Paulo, Brazil) (Souza et al. 2018).

Preparation of fermented biomass

To ferment the biomass, 125 mL Erlenmeyer flasks containing 10 g of cocoa (Theobroma cacao) fruit peel were sterilized in an autoclave (CS30, Prismatec—São Paulo, Brazil) at 121 ºC, 1 atm pressure, for 15 min. Once cooled, the substrate was inoculated with 10^7 spores per gram, and sterile distilled water was added to achieve 60% moisture, as measured by Aqualab (Shimadzu; Barueri, São Paulo, Brazil). The flasks were then incubated at 30 °C for three days in a temperature-controlled bacteriological incubator (SL 222, Solab, Piracicaba, Brazil), according to dos Santos et al. (2016).

Production activated carbon

To evaluate the influence of fermentation on activated carbon characteristics, two samples were prepared: one with fermented biomass and another as a control without fermentation, following the methodology proposed by Gonçalves et al. (2024). Both samples were treated with an activating agent, phosphoric acid, at a ratio of 2.5:1 g/g for 48 h at 105 °C in an oven (TE 393/1, Tecnal, São Paulo, Brazil). Subsequently, they were carbonized at 500 °C under a nitrogen flow of 50 mL/min for 1 h in a muffle furnace (3–550, Vulcan, São Paulo, Brazil). The resulting activated carbons, designated as activated cocoa peel (ACC) and activated cocoa peel with Aspergillus niger (ACCAn), were then washed with deionized water at 60 °C until the pH reached 7.0, signaling the end of the washing process. Finally, the ACC and ACCAn were dried at 105 °C for 24 h in forced air circulation ovens (TE 393/1; Tecnal, São Paulo, Brazil), sieved through a 420 µm mesh, and stored in airtight containers.

Zero charge point

The zero-charge point pH (pHpcz) is defined as the pH at which the carbon surface is neutral. The methodology used is called the "11 points experiment" (Regalbuto and Robles 2004). The procedure consisted of adding 50 mg of ACC and ACCAn samples to 50 mL of 0.10 mol/L sodium chloride solution with pH's variation (1–11) while maintaining constant agitation at 20 rpm (713D, Fisatom, São Paulo, Brazil) at 25 °C for 24 h. At the end of 24 h, the pH was measured (PHS3BW, Bel Engineering, Piracicaba, SP, Brazil) and the pHPCZ corresponded to the range where the final pH remained constant regardless of initial pH.

Immobilization of porcine pancreas lipase enzyme (PPL) on activated carbons

Porcine pancreas lipase (PPL) lipase immobilization

The immobilization procedure followed the method described by Santos et al. (2021). The activated carbon samples (1 g) were submerged in 25 mL of 95% ethanol in beakers for 24 h at room temperature. Subsequently, the activated carbons were washed with distilled water and filtered under vacuum (Prismatec, Itu, SP, Brazil). The wet supports (activated carbon) were added to 19 mL of the enzyme solution prepared with 5 mM sodium phosphate buffer and pH 7, containing enzyme load of 40 mg/g of support and homogenized at 200 rpm (Q816M20, Quimis, Diadema, SP, Brazil) at 25 °C for 12 h (Santos et al. 2021). The biocatalysts immobilized with the PPL were filtered under vacuum (Prismatec, Itu, SP, Brazil) and stored at 4 °C for 24 h before application.

Determination of hydrolytic activity by titrimetric method

The hydrolytic activity was determined according to the titrimetric method (Santos et al. 2021). The substrate was prepared by emulsifying 15 g of low acidity Carbonell olive oil and 45 g of gum Arabic solution (3% w/v). Substrate (5 mL), sodium phosphate buffer solution (5 mL) were added to a concentration of 100 mM and pH 7 in Erlenmeyer flask (125 mL). Subsequently, 0.1 mL of the enzyme solution or the supernatant (resulting from the immobilization process) were added. The hydrolysis reaction was carried out at 37 °C, 240 rpm for 5 min in an Orbital Shaker Shaker (Q816M20, Quimis, Diadema, Brazil). After this period, the reaction was stopped with the addition of 10 mL of a 95% ethanol solution. The concentration of free fatty acids released was quantified by titration with a 30 mM NaOH solution. One unit of lipase activity (IU) was defined as the amount of lipase required to release 1 µmol of fatty acid per minute under the conditions of the assay. All samples were performed in triplicate.

Calculations of immobilization parameters

Protein was determined according to the method of Bradford (1976), using bovine serum albumin (BSA) as the standard protein. Immobilized protein loading (PI) was calculated as follows Eq. (1):

$$PI\left(\frac{mg}{g}\right) = \frac{V * (C_{o-} C_f)}{m} \quad (1)$$

where: PI: immobilized protein; V: solution volume; C_o: initial protein concentration (from the enzyme solution); C_f: final protein concentration (from the supernatant, after immobilization) and m: mass of the immobilized support.

The hydrolytic activity was measured through the equation below Eq. (2):

$$AH\left(\frac{U}{g}\right) = \frac{\left(V_{a-} V_b\right) * M_{(NaOH)} * 1000}{t * m} \quad (2)$$

where: V_a = volume of NaOH in the titrated sample; V_b = volume of NaOH of the titrated blank; $M_{(NaOH)}$ = = molarity of the standardized NaOH solution; t = reaction time; m (enzyme) = amount of the aliquot of the enzyme solution that was used.

To measure the immobilization yield Eq. (3) and the specific activity the equations below were applied (Eq. 4):

$$RI(\%) = \frac{\left(A_{o-} A_f\right) * 100}{A_o} \quad (3)$$

where: A_o: initial activity, A_f: final activity

$$AE(U/mg) = \frac{AH}{PI} \quad (4)$$

where: A: activity specifies; DA: hydrolytic activity and PI: immobilized protein.

Gel electrophoresis analysis

At the end of the immobilization procedure, 20 µL of the supernatant were removed, later added to 5 µL of buffer (glycerol 10% m/v, β-mercaptoethanol 5% m/v, SDS 2.3% m/v, Tris–HCl pH 6.8 0.0625 M), then denatured in a protomic thermocycler for seven minutes and applied to the gel. SDS polyacrylamide gel (12.5% w/v) (Laemmli 1970) was prepared and subjected to a current of 30 mA, with constant voltage for 4 h, in a GE Healthcare mini-gel system (Amersham Pharmacia Biotech, UK). We applied the gel according to (Santos et al. 2021) then the gels were immersed in Coomassie Brilliant Blue and later scanned in a Visioneer One touch scanner (Onetouch 8700, Visioneer, Burlington, USA).

Characterization of the solids used

Porosity measurement and specific surface area

The adsorption and desorption isotherms of activated carbons were obtained in Micromeritcs model ASAP 2420 equipment, using 0.20 g of sample. The samples were submitted to a pre-treatment step, which consisted of heating at 120 ºC. Then the samples were heated to 200 °C, with a

heating rate of 10 °C min^{-1}, remaining for 300 min. Subsequently, nitrogen adsorption and desorption isotherms were obtained at 77 K. The specific surface area was determined by the BET equation (Brunauer et al. 1938). The pore distribution was obtained from the desorption isotherm using the BJH method (Barrett et al. 1951), while the micropore volume was determined by t-plot analysis from the adsorption isotherm (Lippens 1964).

Fourier transform infrared spectroscopy (FTIR)

The functional groups of the free enzyme, activated carbon and biocatalyst, were analyzed by attenuated total reflectance (ATR) in the infrared region of 4000–500 cm^{-1} on a Cary 630 FTIR Mid-Infrared Spectrophotometer (Agilent Technologies Inc, Santa Clara, CA, USA).

X-ray diffractometry (DRX)

Crystallinity was evaluated by X-ray diffraction (XRD) in an XRD-6000 equipment (Shimadzu, Barueri, SP, Brazil) with Cu radiation. $K\alpha = 0.1518$ nm (40 kV, 30 mA), with an angle ranging from $2\theta = 2°–50°$, with a step of 0.05° and an integration time of 2 s. In the powder form, the samples were properly arranged in the sample holder and taken to the radiation chamber (French 2014).

Thermogravimetric analysis (TG/DTG)

Analysis was performed using the DTG-60 series equipment (Shimadzu, Barueri, Brazil). The samples were heated in the range from 30 to 1000 °C, in an inert atmosphere, with a heating rate of 10 °C under a nitrogen flow of 30 mL/min.

Application of biocatalysts in the production of aromas from aroma compounds and stability tests of biocatalysts

The synthesis of the apple-citrus aroma ester was carried out in closed Duran flasks with butyric acid and hexanol (1:1 molar ratio) in heptane. The reactions were carried out with the biocatalysts (ACCI and ACCAnI) in the concentration (10% w/v) and reaction medium (butylic acid:hexanol in heptane) under stirring at 200 rpm and 40 °C for 30 h (Q816M20, Quimis, Diadem, Brazil). Reaction progress was determined by removing 200 µL over time to quantify residual butyric acid concentration by titration. Conversion was determined according to Eq. (5) (Alves et al. 2017).

$$\text{Conversion } \% = \frac{A_{(initial)} - A_{(final)}}{AH_{(initial)}} * 100 \quad (5)$$

where: $A_{initial}$ and A_{final} are the initial and final fatty acid concentration in the reaction medium (mM).

The operational stability of the biocatalysts was verified by means of hydrolytic reactions in consecutive batches using the same immobilized biocatalyst. 7 cycles were performed and at the end of each one, the biocatalysts were removed from the reaction medium and washed with cold hexane and reused in the next reaction cycle (Alves et al. 2017; Bassi et al. 2016).

Statistical analysis

All analysis were performed in triplicate and the results presented as mean ± standard deviation. Analysis of variance (ANOVA) and Tukey's multiple comparisons, at a 5% significance level, were performed using the Statistical Analysis System (SAS) version 8.0 and Origin Pro 8.0.

Results and discussion

Preparation of activated carbons and zero charge point (pHpcz)

The determination of the zero-charge point (pHpcz) is carried out to delimit the pH ranges in which the surface charges can vary, either positively or negatively. When solutions have pH below the zero-charge point, this indicates that the surface of the coals undergoes protonation, favoring the adsorption of negatively charged proteins. On the other hand, in solutions with pH above the zero-charge point, the adsorption pattern is reversed, as pointed out by Brito et al. (2017).

For this reason, the determination of the pH of zero charge point is a high-relevance parameter to optimize the adsorption efficiency. This occurs due to its influence on the distribution of functional groups in the active sites present on the coal surface, as highlighted by Pereira et al. (2014). Remarkably, the pHpcz values identified in both samples (Fig. 1) were close, remaining around 4.5 and 4.7. This consistency reinforces the formation of acid groups on the activated carbon surface, as suggested by Brito et al. (2017).

Brito et al. (2017), reported zero charge point of activated carbon from cajá core of approximately 5.2 and 5.7, in the samples analyzed. In this work, the activated carbon produced presented higher acidity and thus presented superior surface properties for the adsorption of lipase (Santos et al. 2019). This process can be explained due to the electrostatic attraction between the charge of the coal surface and the anionic group of the lipase (Yao et al. 2016). Therefore, the fermentative process did not interfere with the acidic characteristics of the activated carbon.

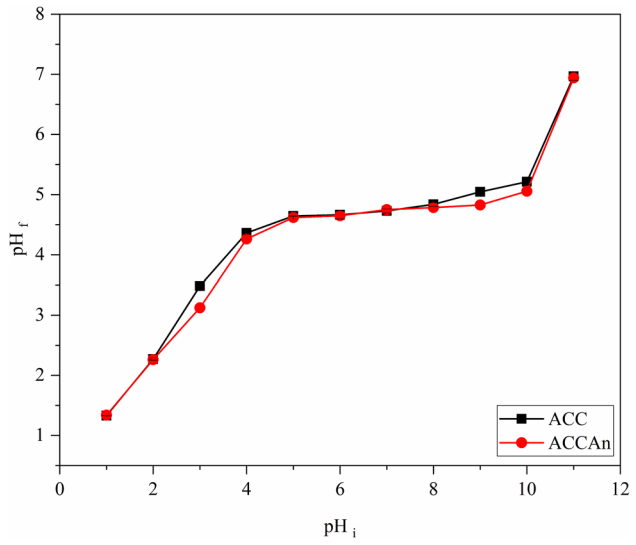

Fig. 1 Determination of pHpcz of activated carbons with phosphoric acid (pH_i, initial value; pH_f, final value)

Immobilization of the lipase enzyme (PPL) on activated carbons

Determination of hydrolytic activity

Solid state fermentation helped in the adsorptive properties of activated carbon (ACCAn). The immobilization parameters were higher, highlighting the 25% increase in the immobilized protein content, in addition to this result, we observed an improvement in other parameters such as Hydrolytic Activity (HA), Yield from immobilization of hydrolytic activity (YIHA) and specific activity (AS) by 11%, 15% and 42%, respectively.

In this study, an enzymatic concentration of 40 mg/g was used, and a hydrolytic activity of 83 U/g was observed for the activated carbon produced from fermented biomass. Conversely, Brito et al. (2017) assessed the enzymatic immobilization on activated carbon with an enzymatic concentration a 100-fold higher (4000 mg/L), noting a peak hydrolytic activity of 278.4 U/g. These results confirm the high affinity of the support produced by the biomass fermented by the lipase enzyme. Therefore, using solid-state fermentation on lignocellulosic residues before the production of activated carbon is a pre-treatment that improves the adsorptive characteristics of the supports and, consequently, the efficiency of the biocatalyst (Gonçalves et al. 2024).

Gel electrophoresis analysis

Electrophoresis analyses were performed on samples of free enzyme, LPP, and supernatants, SACC and SCAAn. The results obtained are presented in Fig. 2.

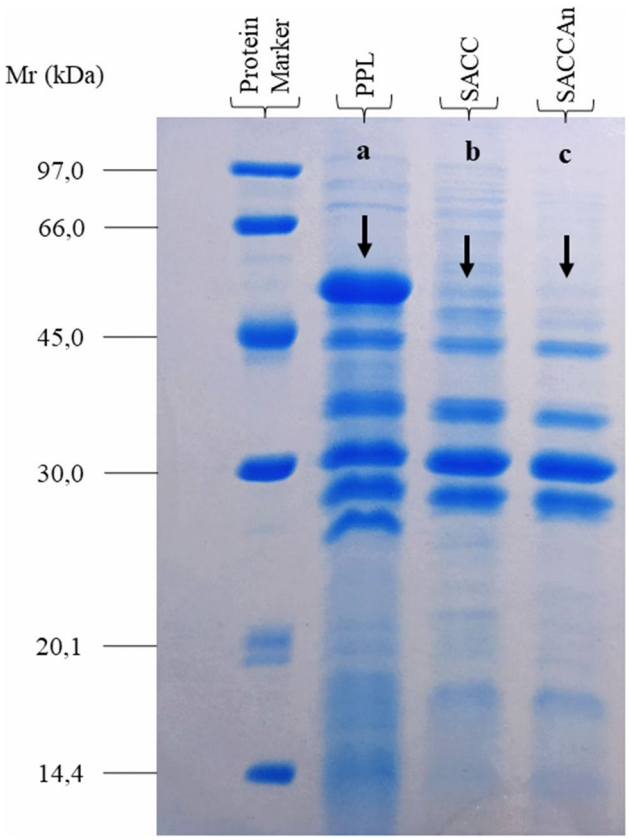

Fig. 2 SDS-PAGE electrophoresis profile of porcine pancreas lipase enzymatic solution (LPP) and Supernatant after immobilization on cocoa husk activated carbon-SACC end Supernatant after immobilization Activated carbon from cocoa shell after SSF with *Aspergillus níger*-SCAAn

In well (a), Fig. 2, it is possible to verify an intense band in the region that can be attributed to the enzyme LPP, since according to Bassi et al. (2016) it is characterized by the molecular weight of 52 kDa. On the other hand, the electrophoresis analyses after the immobilization process, show that there was a reduction of this band in the supernatant samples, wells (b) and (c), which indicates that the enzyme did not desorb from the supports (Neto 2023). It is noteworthy, however, that this reduction in the characteristic band of LPP was more intense in the supernatant of the SCAAn sample. This result suggests that the lipase enzyme was immobilized with greater efficiency on the activated carbon produced after the fermentation process. The data of hydrolytic activity and immobilization yield, Table 1, corroborate the results mentioned, demonstrating that the use of fermented biomass as raw material for the production of activated carbon increases the enzyme adsorption capacity.

Table 1 Immobilization parameters of Porcine Pancreas Lipase (LPP) on different supports: ACC—Activated cocoa husk charcoal, ACCAn—Activated cocoa husk charcoal after SSF with *A. niger* ATCC 1004

Supports	IP (mg/g)	HA (U/g $_{sup}$)	% YIHA $_{sup}$	SA (U/mg)
ACC	19.63 ± 5.78^{c}	75.22 ± 18.13^{c}	83.33 ± 3.97^{c}	2.50 ± 0.27^{b}
ACCAn	24.64 ± 0.62^{a}	83.32 ± 13.59^{a}	95.83 ± 1.56^{a}	3.54 ± 0.45^{a}

IP immobilized protein, *YIHA* yield of immobilization of hydrolytic activity, *HA* hydrolytic activity observed on support, *SA* specific activity in support

The means followed by the same letter in each column do not differ statistically from each other by the Tukey test ($p < 0.05$). Mean values ± standard deviation

Characterization of the utilized solids

Porosity measurement and specific surface area

The nitrogen adsorption/desorption isotherms of activated carbons are shown in Fig. 3. According to the shape, and in accordance with the IUPAC classification (1982), the isotherms can be classified as type IV isotherms, characteristic of mesoporous materials. This type of isotherm indicates the phenomenon of capillary condensation, characteristic of materials in which the formation of a monolayer on the surfaces is followed by a multilayer adsorption until the point of inflection and saturation of the isotherm (Brito et al. 2020a; b).

The first slope, which occurs at low p/p0 values, corresponds to monolayer coverage, while the second slope shows adsorption and capillary condensation. These results suggest that hysteresis cycle isotherms are wider at high relative pressures and correspond to a mixed structure of the material, consisting of micropores and mesopores, as evaluated in activated carbon by Kumar and Jena (2016). In an adsorption process, it is desirable that the adsorbent has a good interaction between mesopores and micropores, as the mesopores can allow rapid diffusion of molecules within the coals and access to the micropores, where the adsorption occurs to a large extent (Santos et al. 2020).

The carbon produced from the fermented biomass, ACCAn, adsorbed approximately 15% more N_2 than the ACC sample (Fig. 3a). This result demonstrates that the fermentation favored the formation of bulky pores and consequently high surface area (Brito et al. 2020a; b). Table 2 confirms and presents in detail the textural and physical characteristics of the synthesized adsorbents. It is observed that the activated carbons ACC and ACCAn exhibited a high surface area (1084.69 m^2/g and 1107.87 m^2/g, respectively, due to the origin of the raw material and the activation mechanism with phosphoric acid. It is worth noting that the fermentation process increased the surface area and the pore volume by 10%. During fermentation, microorganisms promote the degradation of lignin, which improves the carbonization process, reducing the

Table 2 Textural properties of the ACC—Activated cocoa husk charcoal, ACCAn—Activated cocoa husk charcoal after SSF with *A. niger* ATCC 1004

Supports	Surface area (m^2/g)	Pore diameter (nm)	Pore volume (cm^3/g)
ACC	1084.69	3.62	0.477
ACCAn	1107.87	3.63	0.525

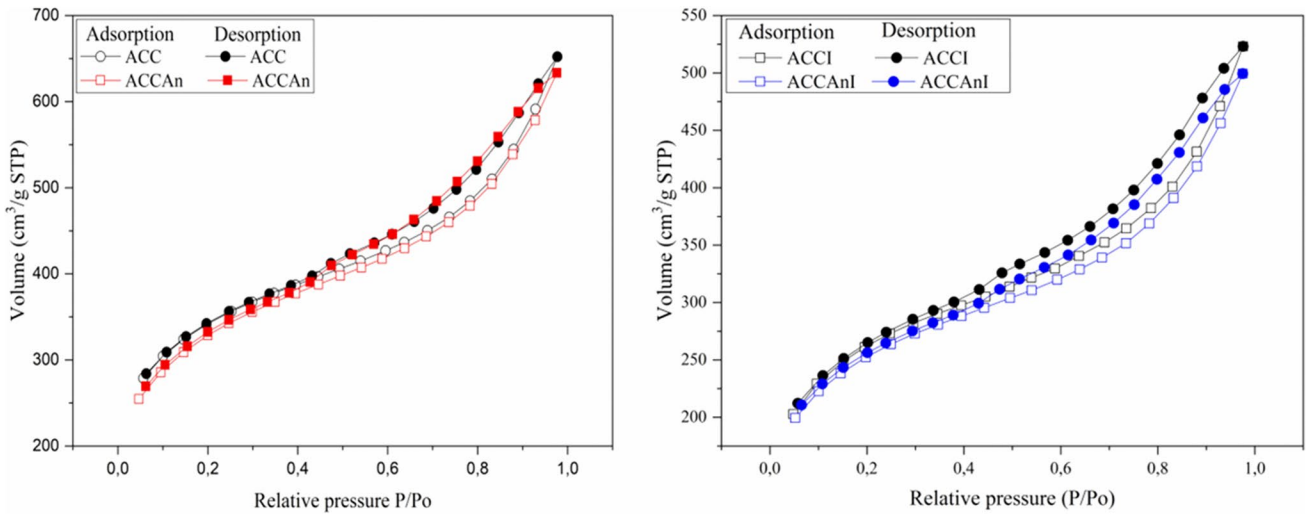

Fig. 3 Nitrogen adsorption isotherms of activated carbon ACC—Activated cocoa husk charcoal, ACCAn—activated cocoa husk charcoal after SSF with *A. níger* ATCC 1004

lignin content which hinders the thermal degradation process (Santos et al. 2020).

The results of this study demonstrated significant superiority compared to previous studies conducted by Samanta et al. (2020) and León et al. (2022) regarding the surface area of the analyzed material. Samanta et al. (2020) achieved a surface area of 962 m^2/g, employing phosphoric acid as the activating agent, while León et al. (2022) obtained 969 m^2/g using cocoa shell as the precursor materia.

However, there was no significant difference in the pore diameter. The explanation for the increase in surface area and pore volume regardless of the diameter may be related to the increase in their depth. The direct effect of depth is observed in the increase of the immobilization parameters presented in Table 1 when using the biocatalyst obtained after the fermentation process (Gonçalves et al. 2024).

Fourier transform infrared spectroscopy (FTIR-ATR)

The FTIR-ATR spectra of cocoa husk samples (Fig. 4a), activated carbons (Fig. 4b) and immobilized biocatalysts (Fig. 4b) showed chemical changes on the surface of the matrices after residue activation and enzymatic immobilization.In samples A (Fig. 4a) absorption peaks were identified. The most intense band that appears at 3293 cm^{-1} can be attributed to a stretching of the hydroxyl functional groups (–OH), belonging to the cellulose structure (Brito et al. 2017). Characteristic groups of lignocellulosic materials are evidenced by bands in the region of 2923 and 2310 cm^{-1} resulting from the axial deformation of bonds (C–H) characteristic of the compounds cellulose, lignin and hemicellulose. The degradation of these compounds can be observed as a function of the reduction in the intensity of these bands (Fig. 4a), as proposed by Pereira et al. (2014). The band in the region of 1603 cm^{-1} is representative of typical stretches

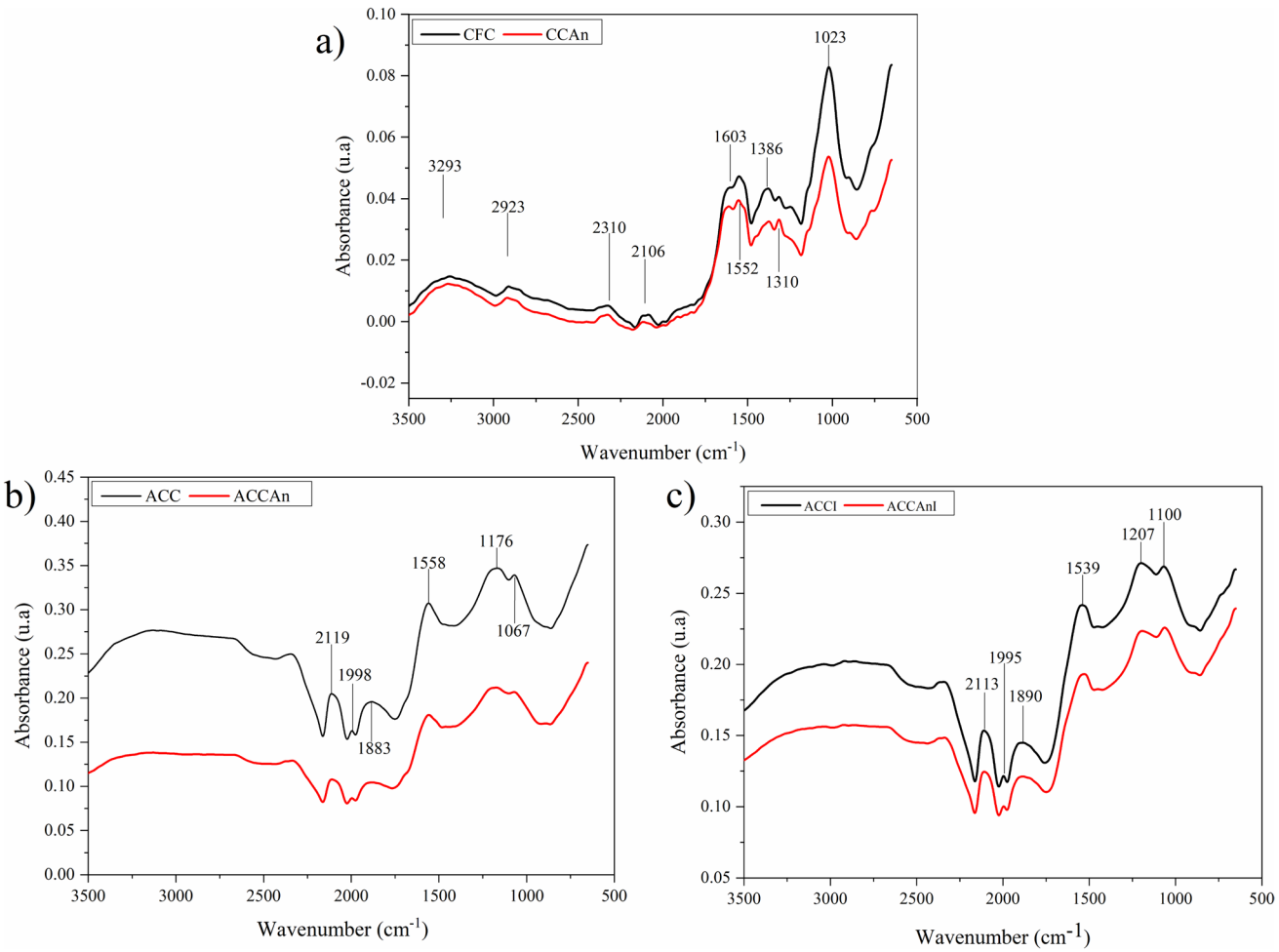

Fig. 4 FTIR of CFC—Cocoa husk residue without SSF, CCAn—Cocoa husk residue after SSF with *A niger* ATCC 1004, ACC—activated charcoal from cocoa husk without SSF, ACCAn—activated charcoal from cocoa husks after SSF with *A. niger* ATCC 1004, ACCI—activated charcoal from cocoa husk with immobilized PPL, ACCAnI – Activated charcoal from cocoa husks after SSF with *A. niger* ATCC 1004 with immobilized PPL

of aromatic compounds (C–C). In addition to these, it is also worth mentioning the band in the region of 1023 cm^{-1} attributed to stretching of glycosidic bonds (C–O–C) present in cellulose and hemicellulose (Moretti et al. 2014; Santos et al. 2020).

The samples CFC and CCAn (Fig. 4a) and ACC and ACCAn (Fig. 4b) showed spectra that indicate changes in functional groups in the region 2923 and 2310 (C–H) and 1603 cm^{-1} (C–C) present in the residues before carbonization, when compared with the activated carbons obtained. After the activation process, there was a reduction of several functional groups, among them those that are related to the C–H and C–C groups, due to the decomposition of the organic matter present in the residues (Kan et al. 2017).

The samples ACCI and ACCAn (Fig. 5c.) in the regions between 3000 and 2500 cm^{-1} showed changes that correspond to the overlap of carbon stretching with stretching of lipase NH groups. The pronounced bands at 1100 cm^{-1}, which are attributed to the vibrations of the CN bonds characteristic of the amino groups present in lipase, were identified by Almeida et al. (2017) and also observed by Brito et al. (2020a; b) in their study of lipase immobilized on activated carbon produced from the sheath of the peach palm.

X-ray diffractometry (DRX)

The crystallinity of the samples used was determined using the X-Ray Diffractometry (XRD) technique, as shown in Fig. 5. The diffractograms corresponding to the CFC and CCAn samples (Fig. 5a) showed that the materials have a predominantly amorphous characteristic, with two typical peaks of an amorphous halo situated between the angles $15° \leq 2\theta \geq 22°$, making it possible to infer that intermolecular interferences occur due to the degree of packaging of

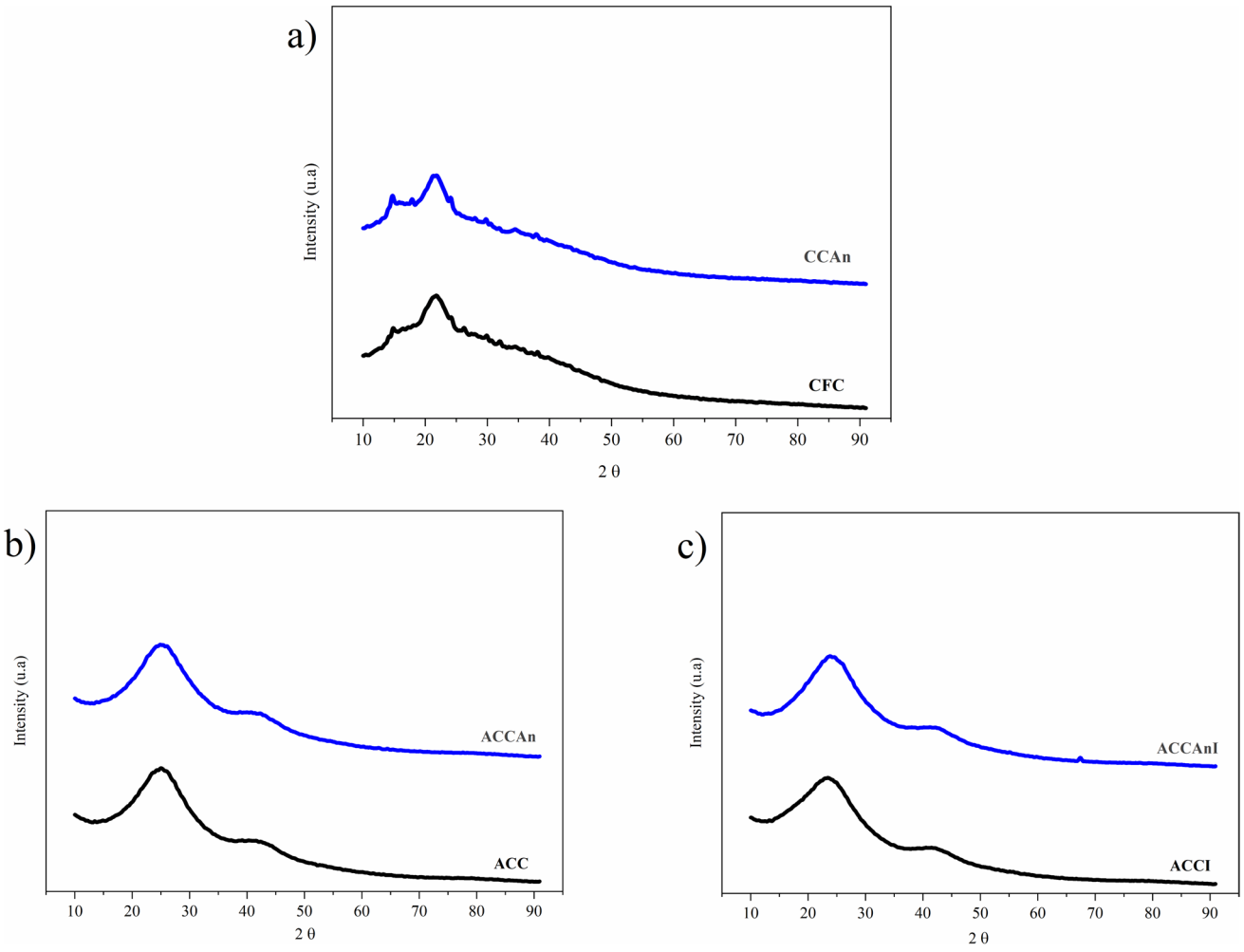

Fig. 5 XRD diffractogram: CFC—Cocoa husk residue without SSF, CCAn—Cocoa husk residue after SSF with *A. niger* ATCC 1004, ACC—activated charcoal from cocoa husk without SSF, ACCAn—activated charcoal from cocoa husks after SSF with *A. niger* ATCC 1004, ACCI—activated charcoal from cocoa husk with immobilized PPL, ACCAnI—activated charcoal from cocoa husks after SSF with *A. niger* ATCC 1004 with immobilized PPL

molecules in the amorphous phase (Guilhen et al. 2019). In the literature, it is recognized that XRD patterns of biomass are characterized by intense amorphous halo with maximum values between 2θ = 20° and 23°, mainly indicating the presence of cellulose and minimum values between 2θ = 13° and 17°, related to the occurrence of lignin. The observed smoothness in the diffractograms of the fermented biomass may be associated with the material's degradation during the solid-state fermentation (SSF) process, as suggested by Vassilev et al. (2013).

The supports (carbons) and biocatalysts evaluated were shown to be similar by X-ray diffraction analysis (Fig. 5b and c). Amorphous activated carbon is commonly composed of small crystalline regions resulting from its graphitic structure. In addition, amorphous halos that stand out in the diffractogram, located in the regions of 2θ = 20° and 40°, correspond to carbon, resulting from the activated carbon production phase (McEvoy and Zhang 2014).

However, it is worth emphasizing that materials produced from lignocellulosic residues, which present a higher concentration of cellulose and lignin in their composition, tend to result in amorphous materials (Santos et al. 2020), as verified in this study using the husk of the cocoa fruit.

Thermogravimetric analysis (TG/DTG)

To evaluate the changes in thermal stability that occurred during the carbonization process of the raw material impregnated with phosphoric acid, thermal analyzes were carried out using thermogravimetry (Fig. 6).

In region I of Fig. 6a, we observed a mass loss of approximately 10%, 20% and 25% for the CFC, ACCI and ACC

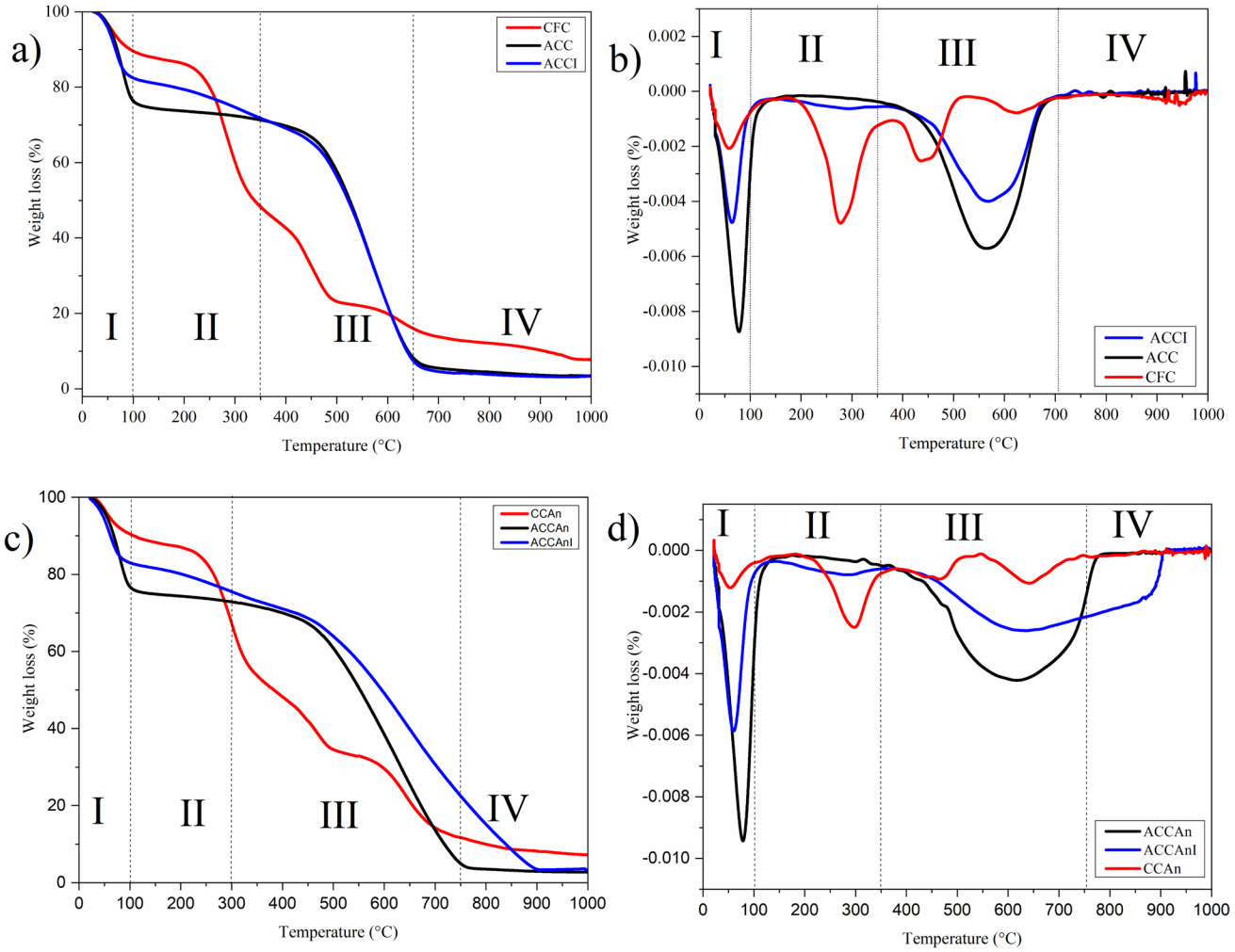

Fig. 6 Thermogravimetric analysis: CFC—Cocoa husk residue without SSF, CCAn—Cocoa husk residue after SSF with *A niger* ATCC 1004, ACC—activated charcoal from cocoa husk without SSF, ACCAn – activated charcoal from cocoa husks after SSF with *A. niger* ATCC 1004, ACCI—activated charcoal from cocoa husk with immobilized PPL, ACCAnI—activated charcoal from cocoa husks after SSF with *A. niger* ATCC 1004 with immobilized PPL

samples, respectively. According to Pereira et al. (2014), this variation can be attributed to the evaporation of water. Activated carbon immobilized with the enzyme (ACCI) suffered a lower mass loss when compared to ACC, the interaction between water molecules and the enzyme through hydrogen bonds may explain this effect.

In region II (100–350 °C), of the same figure, we observed a marked loss of mass for CFC, a fact that can be attributed to the decomposition of organic matter and the release of volatile compounds (Brito et al. 2020a; b). However, it was observed that after the immobilization of the enzyme (ACCI) the mass loss occurred constantly, ranging from 85 to 70%, that is, having a mass loss of 15%, while the ACC showed no loss of mass in that region. From these data, it can be inferred that enzyme degradation occurred in this region.

In region III, there was a loss of mass related to the decomposition of lignin in the CFC (33%). However, we observed a mass loss of approximately 65% in both activated carbon samples (ACC and ACCI) independent of enzymatic immobilization. In region IV, in the CFC there was a continuous reduction that can be attributed to a prolongation of lignin degradation (Jain et al. 2016) and no loss of mass was observed in the other samples.

In the study conducted by Brito et al. (2020a; b) on activated carbon produced from peach palm sheath, thermal events similar to those studied in this work were observed. This allows us to infer that activated carbons produced from lignocellulosic biomass residues exhibit similar thermal behaviors, differing only in the amount of mass loss observed in the activated carbon produced from fermented biomass.

In the DTG (Fig. 6b), we observed the presence of endothermic peaks in regions I, II and III. Corroborating the events discussed in Fig. 6a.

In region I and II (Fig. 6c), we observed events similar to those discussed in the same region of Fig. 6a. However, in region III of Fig. 6c, we observed a difference in mass loss between ACCAn and ACCAnI. In the ACCAn coal the mass loss was 60%, while in the ACCAnI sample the loss was 45%. We propose that this difference is attributed to the location of enzyme immobilization. Probably the enzyme was immobilized inside the pores when compared to ACCAI (Fig. 6a), the solid-state fermentation process increases the surface area and the pore volume, as we observed in the BET analysis. Consequently, it is necessary to raise the temperature for the degradation of compounds inside the pores.

In region IV, ACCAnI, we observed a continuous loss of mass (15%), we can infer that there is a continuous degradation of organic compounds. The other samples do not show mass loss in this region.

In Fig. 5d, we observe the appearance of endothermic peaks of greater intensity in region I, II, III. These results confirm the results discussed earlier in Fig. 6c. In region IV, the endothermic peak is only apparent for the ACCAnI samples, corroborating the results in Fig. 6c.

Application of biocatalysts in aroma production

The biocatalyst was used in the production of hexyl butyrate and the results can be seen in Fig. 7. The biocatalyst produced after fermentation (ACCAnI) showed a maximum conversion of 40% in just 8 min of reaction, while the ACCI had a maximum conversion of 32% after 15 min. It is noteworthy that in addition to needing twice as much time, production was 25% lower compared to the ester synthesized with the biocatalyst produced from fermented biomass. These results demonstrate that the solid-state fermentation process favored the production of aromas.

Santos et al. (2021) synthesized the hexyl butyrate ester using the Diaion HP 20 support immobilized with the lipase enzyme from *Mucor javanicus*, *Candida* sp. and *Candida rugosa*, however the production of aromas only started after 20 min of reaction. Brito et al. (2020a; b) produced the aroma of isoamyl acetate using activated carbon from peach palm sheaths and malt bagasse with the enzyme PPL, however only after 1 h the conversion was initiated. Gonçalves et al. (2021), evaluated the synthesis of butyl butyrate using the enzyme PPL immobilized on activated carbon from tamarind seeds and observed the reaction only after 4 h of reaction.

Therefore, we can highlight that the use of fermented biomass as raw material for the production of activated carbon

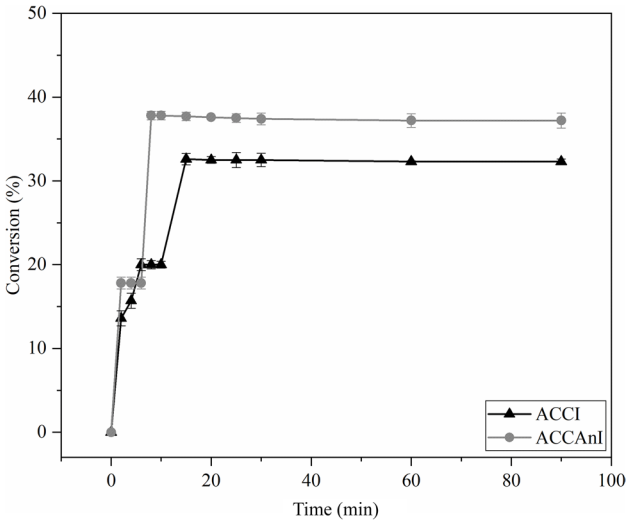

Fig. 7 Esterification yield (%) as a function of time for lipase catalyzed synthesis of hexyl butyrate from pig pancreas immobilized on charcoals ACCI—activated charcoal from cocoa husk with immobilized PPL, ACCAnI—activated charcoal from cocoa husks after SSF with *A. niger* ATCC 1004 with immobilized PPL. Values are represented as mean ± standard deviation

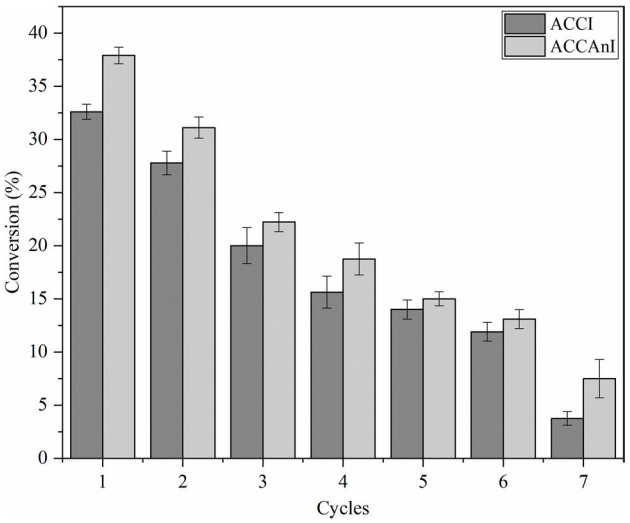

Fig. 8 Biocatalyst reuse tests ACCI—activated charcoal from cocoa husk with immobilized PPL, ACCAnI—activated charcoal from cocoa husks after SSF with *A. niger* ATCC 1004 with immobilized PPL in successive reaction cycles

is efficient in the application of aroma compounds production, as it presented a production time 2.5 times faster than that reported by Santos et al. (2021); 7.5 times faster than the results of Brito et al. (2020a); 30 times faster than those of Gonçalves et al. (2021) and 11 times faster than Todero et al. (2015).

Stability tests of biocatalysts

The operational stability of the biocatalyst was evaluated during seven reuse cycles, and the residual esterification yield was quantified as a function of the number of reuse cycles (Fig. 8).

The ACCAnI biocatalyst, regardless of the cycle, showed the highest amount of hexyl butyrate ester produced. In the first cycle the ACCAnI biocatalyst had a stability of approximately 25% above the ACCI, between the second and sixth cycle the ACCAnI presented a yield of 10% above the ACCI and in the seventh cycle the yield of the ACCAnI was approximately 50% higher when compared with the ACCI.

Toledo et al. (2015), synthesized isoamyl butyrate (banana flavor) using mesoporous polymethacrylate particles as a biocatalyst and obtained a yield of approximately 35% after the seventh cycle. Verissimo et al. (2018) used synthetic support (monolithic cryogel) and achieved a residual esterification yield of butyl butyrate ester (pineapple flavor) of 40% in the fifth reuse cycle. Therefore, we can say that the biocatalyst produced from the fermented biomass was effective in the synthesis of hexyl butyrate ester (apple aroma with citrus), and it can be inferred that the ACCAnI biocatalyst presented the lowest enzymatic leaching.

Conclusion

This research demonstrates that fermented cocoa husk biomass enhances activated carbon production, yielding a biocatalyst with superior adsorptive capacity and enzymatic activity. The activated carbon showed a 25% increase in adsorption and a 10% increase in surface area and pore volume, leading to an 11% higher hydrolytic activity compared to the control. The application in hexyl butyrate synthesis revealed improved conversion rates and operational stability, confirming the potential of fermented biomass for industrial use.

Acknowledgements This study was financed in part by the Fundação de Amparo à Pesquisa do Estado da Bahia (FAPESB) and the National Council for Scientific and Technological Development (CNPq, Brazil) for financial support (308300/2021-1).

Author contributions Conceptualization, M.F., C.M.V., M.S.G., I.M.C.T., M.M.O.S.; methodology, M.F., M.S.G., I.M.C.T., S.C.A., M.M.O.S., C.M.V., A.A.M., P.N.M.A., M.L.O.F.; validation, I.C.F.S., M.S.G., H.L.B.S.A.; writing—original draft preparation, M.S.G., I.M.C.T., I.C.F.S.; writing review and editing, visualization, M.SG., I.M.C.T.; J.L.V.N., P.N.M.A., M.L.O.F., H.A.R., A.A.M., M.F.; supervision, M.F.; project administration, M.F.; All authors have read and agreed to the published version of the manuscript.

Data availability The data presented in this study are available on request from the corresponding author.

Declarations

Conflict of interest The authors declare no conflict of interest. The funders had no role in the design of the study; in the collection, analyses, or interpretation of data; in the writing of the manuscript; or in the decision to publish the results.

References

Almeida LC, Barbosa AS, Fricks AT, Freitas LS, Lima ÁS, Soare CMF (2017) Use of conventional or non-conventional treatments of biochar for lipase immobilization. Process Biochem 61:124–129. https://doi.org/10.1016/j.procbio.2017.06.020

Alves MD, Aracri FM, Cren ÉC, Mendes AA (2017) Isotherm, kinetic, mechanism and thermodynamic studies of adsorption of a microbial lipase on a mesoporous and hydrophobic. Resin Chem Eng J 311:1–12. https://doi.org/10.1016/j.cej.2016.11.069

Arana-Peña S, Carballares D, Morellon-Sterling R, Rocha-Martin J, Fernandez-Lafuente R (2022) The combination of covalent and ionic exchange immobilizations enables the coimmobilization on vinyl sulfone activated supports and the reuse of the most stable immobilized enzyme. Int J Biol Macromol 199:51–60. https://doi.org/10.1016/j.ijbiomac.2021.12.148

Araujo SC, Ramos MRMF, Santos ELE, de Menezes LHS, de Carvalho MS, Tavares IMC, Franco M, de Oliveira JR (2022) Optimization of lipase production by *Penicillium roqueforti* ATCC 10110 through solid-state fermentation using agro-industrial residue based on a univariate analysis. Prep Biochem Biotechnol 52(3):325–330. https://doi.org/10.1080/10826068.2021.1944203

Barbosa O, Torres R, Ortiz C, Berenguer-Murcia Á, Rodrigues RC, Fernandez-Lafuente RH (2013) Eterofunctional supports in enzyme immobilization: from traditional immobilization protocols to opportunities in tuning enzyme properties. Biomacromol 14:2433–2462. https://doi.org/10.1021/bm400762h

Barrett EP, Joyner LG, Halenda PP (1951) The determination of pore volume and area distributions in porous substances. I. Computations from nitrogen isotherms. J Am Chem Soc 73:373–380. https://doi.org/10.1021/ja01145a126

Bassi JJ, Todero LM, Lage FAP, Khedy GI, Ducas JD, Custódio AP, Pinto MA, Mendes AA (2016) Interfacial activation of lipases on hydrophobic support and application in the synthesis of a lubricant ester. Int J Biol Macromol 92:900–909. https://doi.org/10.1016/j.ijbiomac.2016.07.097

Bradford MM (1976) Rapid and sensitive method for the quantitation of microgram quantities of protein utilizing the principle of protein-dye binding. Anal Biochem 72:248–254. https://doi.org/10.1016/0003-2697(76)90527-3

Brito MJP, Veloso CM, Bonom RCF, Fontan RCI, Santo LS, Monteiro KA (2017) Activated carbons preparation from yellow mombin fruit stones for lipase immobilization. Fuel Process Technol 156:421–428. https://doi.org/10.1016/j.fuproc.2016.10.003

Brito MJP, Bauer LC, Santos MPF, Santos LS, Bonomo RCF, Fontan RCI, Veloso CM (2020a) Lipase immobilization on activated and functionalized carbon for the aroma ester synthesis. Microporous Mesoporous Mater 309:110576. https://doi.org/10.1016/j.micromeso.2020.110576

Brito MJP, Flores MPS, Souza ECJ, Santos LS, Bonomo RCF, Costa Fontan RI, Veloso CM, Brito MJP, Santos MPF, Veloso CM (2020b) Development of activated carbon from pupunha palm heart sheaths: effect of synthesis conditions and its application in lipase immobilization. J Environ Chem Eng 8:104391. https://doi.org/10.1016/j.jece.2020.104391

Brunauer S, Emmett PH, Teller E (1938) Adsorption of gases in multimolecular layers. J Am Chem Soc 60:309–319. https://doi.org/10.1021/ja01269a023

Carvalho MS, Menezes LHS, Pimentel AB, Costa FS, Oliveira PC, Santos MMO, Tavares IMC, Irfan M, Bilal M, Dias JCT, Oliveira JR, Franco M (2023) Application of chemometric methods for the optimization secretion of xylanase by *Aspergillus oryzae* in solid state fermentation and its application in the saccharification of agro-industrial waste. Waste Biomass Valor 14:3183–3193. https://doi.org/10.1007/s12649-022-01832-8

Costa-Silva TA, Carvalho AKF, Souza CRF et al (2022) Highly effective Candida rugosa lipase immobilization on renewable carriers: Integrated drying and immobilization process to improve enzyme performance. Chem Eng Res Des 183:41–55. https://doi.org/10.1016/j.cherd.2022.04.026

FAO (2020) World food and agriculture - statistical yearbook 2020. Food and Agriculture Organization of the United Nations, Rome, Italy

Ferraz JLAA, Souza LO, Fernandes AAG, Oliveira MLFO, Oliveira JR, Franco M (2019) Optimization of the solid-state fermentation conditions and characterization of xylanase produced by *Penicillium roqueforti* ATCC 10110 using yellow mombin residue (*Spondias mombin* L). Chem Eng Commun 207(1):31–42. https://doi.org/10.1080/00986445.2019.1572000

French AD (2014) Idealized powder diffraction patterns for cellulose polymorphs. Cellulose 21:885–896. https://doi.org/10.1007/s10570-013-0030-4

Gama RS, Bolin ICA, Cren ÉC, Mendes AA (2019) A novel functionalized SiO2-based support prepared from biomass waste for lipase adsorption. Mater Chem Phys 234:146–150. https://doi.org/10.1016/j.matchemphys.2019.06.002

Gonçalves GR, Gandolfi OR, Bonomo RCF, Fontan RCI, Veloso CM (2021) Synthesis of activated carbon from hydrothermally carbonized tamarind seeds for lipase immobilization: characterization and application in aroma ester synthesis. J Chem Technol Biotechnol 96:3316–3329. https://doi.org/10.1002/jctb.6884

Gonçalves MS, Oliveira PC, Araujo SC, Santos ELE, Neta JL, Anjos PN, Ferreira MLO, Salay LC, Sampaio ICF, Santos MMO, Irfan M, Oliveira JR, Franco M (2024) Innovating in the production of activated carbon through the reuse of fermented biomass. Chem Papers. 78:2681–2685. https://doi.org/10.1007/s11696-023-03227-y

Guilhen SN, Mašek O, Ortiz N, Izidoro JC, Fungaro DA (2019) 2 Pyrolytic temperature evaluation of macauba biochar for uranium adsorption from aqueous solutions. Biomass Bioenergy 122:381–390. https://doi.org/10.1016/j.biombioe.2019.01.008

Jain A, Balasubramanian R, Srinivasan MP (2016) Hydrothermal conversion of biomass waste to activated carbon with high porosity: a review. Chem Eng J 283:789–805. https://doi.org/10.1016/j.cej.2015.08.014

Kan Y, Yue Q, Li D, Wu Y, Gao B (2017) Preparation and characterization of activated carbons from waste tea by H3PO4 activation in different atmospheres for oxytetracycline removal. J Taiwan Inst Chem Eng 71:494–500. https://doi.org/10.1016/j.jtice.2016.12.012

Khanna P, Chopra R, Garg M (2021) Laws impacting chemicals added to food. Food Chem. https://doi.org/10.1002/9781119792130.ch4

Kumar A, Jena HM (2016) Preparation and characterization of high surface area activated carbon from Fox nut (*Euryale ferox*) shell by chemical activation with H3PO4. Results Phys 6:651–658. https://doi.org/10.1016/j.rinp.2016.09.012

Laemmli UK (1970) Cleavage of structural proteins during the assembly of the head of bacteriphoge T4. Nature 227:680–685. https://doi.org/10.1038/227680a0

León AY, Rincón JR, Rodríguez N, Molina DR (2022) Optimization of the preparation conditions for cocoa shell-based activated carbon and its evaluation as salts adsorbent material. Int J Environ Sci Technol 19:7777–7790. https://doi.org/10.1007/s13762-021-03687-3

Lessa OA, Silva FN, Tavares IMC, Sampaio ICF, Pimentel AB, Leite SGF, Gutarra MLE, Tienne LGP, Irfan M, Bilal M, Anjos PNM, Salay LCM, Franco M (2023) Structural alteration of cocoa bean shell fibers through biological treatment using *Penicillium roqueforti*. Prep Biochem Biotechnol 53(9):1154–1163. https://doi.org/10.1080/10826068.2023.2177866

Liang Z, Zhang P, Zeng X-A, Fang Z (2021) The art of flavored wine: tradition and future. Trends Food Sci Technol 116:130–145. https://doi.org/10.1016/j.tifs.2021.07.020

Lippens B (1964) Studies on pore systems in catalysts I. The adsorption of nitrogen; apparatus and calculation. J Catal 3:32–37. https://doi.org/10.1016/0021-9517(64)90089-2

Lizardi-Jiménez MA, Hernández-Martínez R (2017) Solid state fermentation (SSF): diversity of applications to valorize waste and biomass. 3 Biotech. https://doi.org/10.1007/s13205-017-0692-y

Lu F, Rodriguez-Garcia J, Van Damme I, Westwood NJ, Shaw L, Robinson JS, Warren G, Chatzifragkou A, McQueen Mason S, Gomez L, Faas L, Balcombe K, Srinivasan C, Picchioni F, Hadley P, Charalampopoulos D (2018) Valorisation strategies for cocoa pod husk and its fractions. Curr Opin Green Sustain Chem 14:80–88. https://doi.org/10.1016/j.cogsc.2018.07.007

Markets and Markets (2022) Flavors & Fragrances Market by Ingredients (Natural, Synthetic), End use (Beverage, Savory & Snacks, Bakery, Dairy Products, Confectionery, Consumer Products, Fine Fragrances), and Region (Asia Pacific, North America, Europe)—Global Forecast to 2026. Northbrook

McEvoy JG, Zhang Z (2014) Synthesis and characterization of magnetically separable Ag/AgCl–magnetic activated carbon composites for visible light induced photocatalytic detoxification and

disinfection. Appl Catal B Environ 160–161:267–278. https://doi.org/10.1016/j.apcatb.2014.04.043
Mendes AA (2019) Enzymatic synthesis of geranyl butyrate via esterification catalyzed by lipase immobilized on a hydrophobic support. J Eng Exact Sci. https://doi.org/10.18540/jcecvl5iss4pp0385-0391
Menezes LH, Carneiro LL, Tavares IMC, Santos PH, Chaga TP, Mendes AA, Silva EGP, Franco M, Oliveira JR (2021) Artificial neural network hybridized with a genetic algorithm for optimization of lipase production from *Penicillium roqueforti* ATCC 10110 in solid-state fermentation. Biocatal Agric Biotechnol 31:101885. https://doi.org/10.1016/j.bcab.2020.101885
Menezes LHS, Ramos MRMF, Araujo SC, Santo ELE, Oliveira PC, Tavares IMC, Santos PH, Franco M, Oliveira JR (2022a) Application of a constrained mixture design for lipase production by *Penicillium roqueforti* ATCC 10110 under solid-state fermentation and using agro-industrial wastes as substrate. Prep Biochem Biotechnol 52(8):885–893. https://doi.org/10.1080/10826068.2021.2004547
Menezes LHS, Santos ELE, Santos MMO, Tavares IMC, Mendes AA, Franco M, Oliveira RJ (2022b) *Candida rugosa* lipase immobilized on hydrophobic support Accurel MP 1000 in the synthesis of emollient esters. Biotechnol Lett 44:89–99. https://doi.org/10.1007/s10529-021-03196-w
Moretti MMS, Bocchini-Martins DA, Nunes CCC, Villena MA, Perrone OM, Silva R, Boscolo M, Gomes E (2014) Pretreatment of sugarcane bagasse with microwaves irradiation and its effects on the structure and on enzymatic hydrolysis. Appl Energy 122:189–195. https://doi.org/10.1016/j.apenergy.2014.02.020
Neto CACG, Prasilde ICM, Silva AS, Silva LMA, Canuto KM, Fontenelle ROS, Rodrigues THS, Rocha MVP (2023) Enzymatic synthesis of citronellyl butyrate by lipase B from *Candida antarctica* immobilized on magnetic cashew apple bagasse lignin. Process Biochem 131:244–255. https://doi.org/10.1016/j.procbio.2023.06.025
Neves CA, Menezes LHS, Soares GA, Reis NS, Tavares IMC, Franco M, Oliveira JR (2022) Production and biochemical characterization of halotolerant β-glucosidase by *Penicillium roqueforti* ATCC 10110 grown in forage palm under solid-state fermentation. Biomass Conv Bioref 12:3133–3144. https://doi.org/10.1007/s13399-020-00930-8
Nogueira LS, Tavares IMC, Santana NB, Ferrão SPB, Teixeira JM, Costa FS, Silva TP, Pereira HJV, Irfan M, Bilalm M, Oliveiram JR, Franco M (2022) Thermostable trypsin-like protease by *Penicillium roqueforti* secreted in cocoa shell fermentation: production optimization, characterization, and application in milk clotting. Biotechnol Appl Biochem 69(5):2069–2080. https://doi.org/10.1002/bab.2268
Nunes NS, Carneiro LL, Menezes LHS, Carvalho MS, Pimentel AB, Silva TP, Pacheco CSV, Tavares IMC, Santos PH, Chagas TP, Silva EGP, Oliveira JR, Bilal M, Franco M (2020) Simplex-centroid design and artificial neural network-genetic algorithm for the optimization of exoglucanase production by *Penicillium roqueforti* ATCC 10110 through solid-state fermentation using a blend of agroindustrial wastes. Bioenergy Res 13:1130–1143. https://doi.org/10.1007/s12155-020-10157-0
Oliveira PC, Brito AR, Pimentel AB, Soares GA, Pacheco CSV, Santana NB, Silva EGP, Fernandes AGA, Ferreira MLO, Oliveira JR, Franco M (2018) Cocoa shell for the production of endoglucanase By *Penicillium roqueforti* ATCC 10110 in solid state fermentation and biochemical properties. Rev Mex Ing Qum 18:777–787
Pereira RG, Veloso CM, Silva NM, Sousa LF, Bonomo RCF, Souza AO, Souza MOG, Fontan RCI (2014) Preparation of activated carbons from cocoa shells and siriguela seeds using H3PO4 and ZnCL2 as activating agents for BSA and α-lactalbumin adsorption. Fuel Process Technol 126:476–486. https://doi.org/10.1016/j.fuproc.2014.06.001
Regalbuto JR, Robles J (2004) The engineering of Pt/carbon catalyst preparation. University of Illinois, Chicago
Reis NS, Santana NB, Tavares IMC, Lessa OA, Santos LR, Pereira NE, Soares GA, Oliveira RA, Oliveira JR, Franco M (2020) Enzyme extraction by lab-scale hydrodistillation of ginger essential oil (*Zingiber officinale* Roscoe): chromatographic and micromorphological analyses. Ind Crops Prod 146:112210. https://doi.org/10.1016/j.indcrop.2020.112210
Ruiz M, Plata E, Castillo JJ, Ortiz CC, López G, Baena S, Torres R, Fernandez-Lafuente R (2021) Modulation of the biocatalytic properties of a novel lipase from psychrophilic *Serratia* sp (USBA-GBX-513) by different immobilization strategies. Mol 26:1574. https://doi.org/10.3390/molecules26061574
Sá AGA, Meneses AC, Araújo PHH, Oliveira D (2017) A review on enzymatic synthesis of aromatic esters used as flavor ingredients for food, cosmetics and pharmaceuticals industries. Trends Food Sci Technol 69:95–105. https://doi.org/10.1016/j.tifs.2017.09.004
Samanta S, Chowdhury S, Daharma D, Halder G (2020) The biosorptive uptake of enrofloxacin from synthetically produced contaminated water by tamarind seed derived activated carbon. RSC Adv 10:1204–1218. https://doi.org/10.1920/bab.1959
Santos TC, Cavalcanti IS, Bonom RCF, Santana NB, Franco M (2011) Optimization of productions of cellulolytic enzymes by *Aspergillus niger* using residue of mango a substrate. Ciên Rural 41(1):2210–2216. https://doi.org/10.1590/S0103-84782011005000145
Santos TC, Reis NS, Silva TP, Machado FPP, Bonomo RCF, Franco M (2016) Prickly palm cactus husk as a raw material for production of ligninolytic enzymes by *Aspergillus niger*. Food Sci Biotechnol 25:205–211. https://doi.org/10.1007/s10068-016-0031-9
Santos MP, Brito MJ, Junior EC et al (2019) Pepsin immobilization on biochar by adsorption and covalent binding, and its application for hydrolysis of bovine casein. J Chem Tech Biotech 94:1982–1990. https://doi.org/10.1002/jctb.5981
Santos MPF, Silva JF, Fontan RCI, Bonomo RCF, Santo LS, Veloso CM (2020) New insight about the relationship between the main characteristics of precursor materials and activated carbon properties using multivariate analysis. Can J Chem Eng 98:1501–1511. https://doi.org/10.1002/cjce.23721
Santos MMO, Gama RS, Tavares IMC, Santos PH, Gonçalves MS, Carvalho MS, Vilas Boas EVB, Oliveira JR, Mendes AA, Franco M (2021) Application of lipase immobilized on a hydrophobic support for the synthesis of aromatic esters. Biotechnol Appl Biochem 68:538–546. https://doi.org/10.1002/bab.1959
Selo G, Planini M, Tišma M, Tomas S, Koceva Komleni D, Bucic-Koji AA (2021) Comprehensive review on valorization of agro-food industrial residues by solid-state fermentation. Foods 10:927. https://doi.org/10.3390/foods10050927
Silva TP, Souza LO, Reis NS, Assis SA, Ferreira MLO, Oliveira JR, Aguiar-Oliveira E, Franco M (2017) Cultivation of *Penicillium roqueforti* in cocoa shell to produce and characterize its lipase extract. Ver Mex Ing Quím 16(3):745–756
Soares GA, Alnoch RC, Dias GS, Reis NDS, Tavares IMC, Ruiz HA, Bilal M, Oliveira JR, Krieger N, Franco M (2022) Production of a fermented solid containing lipases from *Penicillium roqueforti* ATCC 10110 and its direct employment in organic medium in ethyl oleate synthesis. Biotechnol Appl Biochem 69(3):1284–1299. https://doi.org/10.1002/bab.2202
Souza LO, Brito AR, Bonomo RCF, Santana NB, Ferraz JLAA, Aguiar-Oliveira E, Fernandes AGA, Ferreira MLO, Oliveira JR, Franco M (2018) Comparison of the biochemical properties between the xylanases of Thermomyces lanuginosus (Sigma®) and excreted by *Penicillium roqueforti* ATCC 10110 during the solid state fermentation of sugarcane bagasse. Biocatal Agric

Biotechnol 16:277–284. https://doi.org/10.1016/j.bcab.2018.08.016

Todero LM, Bassi JJ, Lage FAP, Corradini MCC, Barboza JCS, Hirata DB, Mendes AA (2015) Enzymatic synthesis of isoamyl butyrate catalyzed by immobilized lipase on poly-methacrylate particles: optimization, reusability and mass transfer studies. Bioprocess Biosyst Eng 38:1601–1613. https://doi.org/10.1007/s00449-015-1402-y

Vassilev SV, Baxter D, Andersen LK, Vassileva CG (2013) An overview of the composition and application of biomass ash. Part 1. Phase–mineral and chemical composition and classification. Fuel 105:40–76. https://doi.org/10.1016/j.fuel.2012.09.041

Veloso MCRA, Pires MR, Villela LS, Scatolino MV, Protásio TP, Mendes LM, Guimarães Júnior JB (2020) Potential destination of Brazilian cocoa agro-industrial wastes for production of materials with high added value. Waste Manag 118:36–44. https://doi.org/10.1016/j.wasman.2020.08.019

Veríssimo LA (2018) Development of a bioreactor based on lipase entrapped in a monolithic cryogel for esterification and interesterification reactions. Rev Mex Ing Quím 17:177–187. https://doi.org/10.24275/uam/izt/dcbi/revmexingquim/2018v17n1/Verissimo

Voukkali I, Papamichae I, Economou F, Loizia P, Klontza E, Lekkas DF, Naddeo V, Zorpas AA (2023) Factors affecting social attitude and behavior for the transition towards a circular economy. Sustain Chem Pharm 36:101276. https://doi.org/10.1016/j.scp.2023.101276

Yao S, Zhang J, Shen D, Xiao R, Gu S, Zhao M, Liang J (2016) Removal of Pb(II) from water by the activated carbon modified by nitric acid under microwave heating. J Colloid Interface 463:118–127